ORIGINAL ARTICLE

Green Synthesis Characterization and Antimicrobial Activity Evaluation of Manganese Oxide Nanoparticles and Comparative Studies with Salicylalchitosan Functionalized Nanoform

M. Muhamed Haneefa[1], M. Jayandran[2], V. Balasubramanian[1]

[1]Department of Chemistry, AMET University, Chennai, Tamil Nadu, India, [2]Department of Chemistry, Thiruvalluvar Government Arts College, Namakkal, Tamil Nadu, India

Abstract

Aim: In this study, we have demonstrated the synthesis of manganese metal oxide nanoparticles (NPs) by a green synthesis manner using lemon extract as a reducing agent and turmeric curcumin extract as capping agent. The as-synthesized nanomaterials were biofunctionalized with salicylalchitosan which was obtained from the source of chitosan to enhance the antimicrobial activity of those materials. **Materials and Methods:** The synthesized materials were characterized using ultraviolet-visible and Fourier transform infrared spectroscopic techniques. Scanning electron microscopy and transmission electron microscopy analysis were employed to evaluate the morphological and structural properties of the both synthesized nanoforms. Furthermore, the effect of antibacterial and antifungal activity of those materials was analyzed using some standard Gram-positive and Gram-negative bacteria and funguses. **Results:** The morphological studies represented that both non-functionalized and biofunctionalized manganese oxide NPs (MONPs) formed are of spherical morphology but exhibited with difference in size about 50 nm and 40-60 nm, respectively. The performance of antimicrobial activity of biofunctionalized MONPs was exhibited better than the non-functionalized NPs. **Conclusion:** The results are revealed that the biofunctionalized MONPs showed higher antibacterial and antifungal activities, and our findings from this work have been provided the new way in the potential application of MONPs through a biofunctionalization process in the clinical and drug invention field.

Key words: Biofunctionalization, chitosan, curcumin, deacetylation, demineralization, deproteinization, Gram-positive, Gram-negative, microbes, nanomaterials

INTRODUCTION

The emergence of antibiotic is recognized as a crucial challenge for public health presently due to the severe increasing of infectious diseases. There are a variety of pathogenic microorganisms are found in the clinical field, in which some common closely related species that cause a wide range of diseases and still a significant cause of death, especially in developing countries. Therefore, new strategies are required to find and progress the next generation of drugs or agents to control microbes, which should be effective and inexpensive therapeutic approaches.[1-3]

Nanomaterials are the prominent necessity of the rapidly developing field of nanomedicine and bionanotechnology, and they can offer a new approach to challenge antibiotic-resistance microbes.[4] Several studies have indicated that nanoparticles (NPs) can be used as therapeutic tools in infections, against microbes because of their unique physical, chemical, mechanical, and magnetic properties and these advantageous properties can be attributed to their defined size, shape, and effective biological properties. NPs display completely new or improved properties based on

Address for correspondence:
M. Muhamed Haneefa, Department of Chemistry, AMET University, Chennai, Tamil Nadu, India.
Phone: +91-9965409669. E-mail: honey79101@gmail.com

Received: 17-11-2016
Revised: 10-12-2016
Accepted: 20-12-2016

definite characteristics. As a result, NPs have received great attention in the clinical application to produce a variety of new bactericidal agents.[5,6] In general, size of the bacterial cell is in the micrometer range, while its outer cellular membranes contain pores in the nanometer range. Since the materials at the nanoscale can penetrate into bacterial cells and producing toxic oxygen radicals to damage cell membranes of microbes which results an efficient inhibition of bacterial growth.[7,8]

NPs of metal oxides play a very important role in many areas of chemistry, physics, and materials science. They have been investigated by several workers in the last few years due to their structural aspects, magnetic properties which steered to potential applications in electronic, optical, and mechanical devices based on variable oxidation states.[9] In addition, NP metal oxides are the most promising as they show good antimicrobial properties due to their large surface area to volume ratio which increasing the microbial resistance to metal ions and its non-toxic nature when compared to organic disinfectants. Hence, metal oxide NPs have been attracted by researchers to use in biomedical and pharmaceutical applications as an alternative effective microbial inhibitors.[10]

According to the reports, various metal oxide NPs were investigated in the field of antimicrobial development. As an important functional metal oxide, manganese oxide have attracted the attention of researchers due to their extensive physical, chemical properties which offer wide range of applications such as catalysis, ion exchange, molecular adsorption, energy storage, chemical and biological sensing, water treatment, and imaging contrast agents.[11-14] However, very limited information is available on the antimicrobial properties of manganese metal oxide NPs. In comparison to published reports, magnetic behavioral nanomaterials are attracted the researchers due to their promising applications in antimicrobial field. In our previous works, we have synthesized low-cost nanomaterials possess magnetic behavior in green process manner, and their antimicrobial studies were explored very well.[15] Similarly, manganese oxide NPs (MONPs) are also possesses great magnetic property, particularly, environmental benignity, and low-cost materials.[16] Therefore, in continuation with our work, herein, we provide an in-depth discussion of the recent development of the synthesis of manganese oxides nanomaterials and their application in the field of antimicrobial agents.

Several novel and effective routes have been devoted to prepare manganese oxides nanomaterials with various shapes and excellent properties, such as hydrothermal method,[17] sol-gel synthesis,[18] wet chemical route,[19] pulsed laser deposition method,[20] precursor technique,[21] thermal process,[22] precipitation method,[23] sonochemical method,[24] and microemulsion.[25] However, there are very few reports only available about MONPs preparation in the green synthesis.[26] Synthesis of NPs in the eco-friendly green synthesis method is an increasing focus of current nanotechnology research because of some limitations of chemical synthesis methods include the use of toxic solvents, precursor chemicals, and by-products.[27] Recently, biosynthetic methods employing either biological microorganisms or plants extract[28,29] have emerged as a simple and alternative to conventional synthetic procedures to obtain nanomaterials. However, the critical aspect in the handling of microorganisms is that some of pathogens are more risky and it needs to maintain at particular temperature, pH and other factors for its growth.[30] Therefore, plant extract mediated synthesis process has attracted greatly over the chemical and microbes mediated methods due to its advantageous, unique in shape and size, inexpensive, non-toxicity, and faster rate of synthesis.[31,32]

However, there is a need to develop highly effective NPs that are stable, robust and harmless that are energetic in the destruction of microorganisms. The interaction of NPs with biomolecules is an expanding field of research, which as yet is largely unexplored.[33] Nanomaterials can be very easily functionalized on the surface with synthetic ligands to effect significant change in properties depending on the application at hand. Biofunctionalization has emerged as integration among biotechnology and nanotechnology for developing an environmental benign biological synthesis of nanomaterials, which possess extremely biocompatible and biological recognition ability. In the field of biofunctionalization, the biomaterial is modified to have highly efficient and biocompatible molecules whether permanently or temporarily and the interaction of biomodified material with metallic NPs that have proven themselves to have a considerable range of application in a variety of aspects of biology and medicine. Therefore, biofunctionalization of nanomaterials with suitable bioactive materials can produce the highly durable antimicrobial agents with non-toxicity. Since the NPs are very smaller which are easily incorporated with several biomolecules and provides great antimicrobial effect. However, the selection of active biomolecules to design the functionalized NPs will be a crucial matter in this field.[34-37]

The development of biomaterials using natural polymers is an advanced and promising channel of current research. Chitosan, a versatile hydrophilic polysaccharide, which is produced commercially by deacetylation of chitin. It has been attracted more attention for its unique properties, biocompatible, biodegradable, nonhazardous, and cost-effective.[38] Chitosan is known to be as excellent biofunctional material, well endured by living tissues, particularly, in medicinal field, chitosan films have been employed as curative wound dressing and as scaffolds for tissue and bone engineering. It has a broad antimicrobial spectrum to which Gram-negative, Gram-positive bacteria, and fungi are highly susceptible.[39,40] The reactive functional groups present in chitosan, i.e., amino group and hydroxyl groups, can be readily subjected to chemical derivatization allowing the manipulation of mechanical and solubility properties which resulted in enlarging the biocompatibility.[41]

Based on the above discussion, in this work, we have synthesized MONPs by green synthesis method and as synthesized materials were biofunctionalized with selected biomaterial, salicylalchitosan (SC). In this method, Mn metal salt was reduced by lemon extract. Turmeric curcumin has been used as a capping agent for MONPs. Curcumin (*Curcuma longa*) is well recognized medicinal natural compound derived from turmeric plants. Turmeric has been attributed a number of medicinal properties in the traditional system of medicine due to the presence of curcumin. Curcumin can be acted as effective stabilizing agent and exhibit considerable effectiveness in medicinal activity.[42-44] The investigation of antimicrobial activity of the non-functionalized as well as biofunctionalized MONP was investigated against Gram-positive bacteria (*Staphylococcus aureus* and *Bacillus subtilis*), Gram-negative bacteria (*Escherichia coli* and *Salmonella typhi*), and some funguses (*Candida albicans*, *Curvularia lunata*, *Aspergillus niger,* and *Trichophyton simii*). From the report, there was a good improvement in the activity was observed for biofunctionalized NPs than the non-functionalized NPs against tested bacterial and fungal species.

MATERIALS AND METHODS

All the chemicals and solvents used were of analytical reagent grade and obtained from Merck (India) Ltd. The turmeric sample (BSR-01) was obtained from Agricultural College and Research Institute, Madurai, India, and prawn sample was purchased from local sea food markets in Tuticorin, India. Solutions were prepared with double distilled water.

Collection of lemon extract

Lemon extracts (*Citrus limon*) are rich sources of citric acid and ascorbic acid which is obtained from lemon fruits. The extracts of lemon are low pH which makes it more antibacterial active source in the medicinal field.[45,46] Lemon fruits were purchased from local markets, washed well, and cut into small pieces. The extracts were obtained by squeezing the fruits properly into a cleaned container for the required amount, and the extracts were slightly heated then separated by filtration with Whatman No. 1 filter paper. The filtered extract was collected and stored for the synthesis of NPs.

Extraction of curcumin

Curcumin has been extracted from turmeric in a several methods. However, Soxhlet extraction method is preferred often to extract the curcumin due to its main advantage of simple and continuous process in which the extraction and filtration process is occurring in a single step. According to the method of Manjunath *et al*., 1991,[47] the required amount of dried turmeric (BSR-01) was taken in the soxhlet extraction chamber, and the solvent material 95% ethanol was added to the flask in the ratio of 1:50. The extraction process was continued under reflux about 3 h at 50-60°C. The extraction was carried out until the color of mixture was getting to change to pale yellow color. The extract was filtered and evaporated to dryness. The dried curcumin was collected and recrystallized to pure form.

Isolation of chitosan

The isolation of chitosan from prawn shells was followed according to the method of Brine and Austin, 1981,[48] and Muzzarelli and Jeuniaux, 1986.[49] The three important steps are involving in the isolation of chitosan from prawn sample, those are demineralization, deproteinization and deacetylation. The exoskeletons of collected prawn sample were removed and washed well with distilled water. The sample was kept in the oven to dryness and then dried sample was powdered. The powdered material was first demineralized using 1 M hydrochloric acid for 5-6 h at room temperature. Then, the sample was washed several times by double distilled water and soaked until reach neutral pH. The neutralized material was dried in oven at 60°C and the dried sample was deproteinized with 1 M aqueous sodium hydroxide at 60°C for 5-6 h. The pink colored solution was obtained and washed several times with double distilled water then soaked again until neutral pH. The obtained chitin material was dried in oven at 60°C overnight, and the dried powder was deacetylated with 40% sodium hydroxide for 5-6 h at 60°C. The obtained dirty whit precipitate of chitosan was washed several times and dried in oven at 60°C overnight.

Synthesis of SC

SC synthesis process was carried out by the normal refluxed method in which the isolated chitosan and SC gets condensed together and yielded the preferred product. The dried pure form of 100 mg of chitosan powder was dissolved in 25 ml of acetic acid solution (0.5 M) with constant stirring and kept on a magnetic stirrer for 2-3 h to get complete dissolved solution. A mixture of 10 ml of salicylaldehyde (0.1 M) in ethanol was prepared, and this mixture was added to the above chitosan. The reaction mixture kept on hot magnetic stirrer at 50-60°C for 12 h. Finally, the yellowish green colored precipitate of SC was obtained and filtered. The precipitate was washed with ethanol and distilled water several times and dried under vacuum at 60°C for overnight. It was kept in a desiccator over silica gel for further analyses.[50]

Synthesis of MONPs

In a typical reaction procedure, manganese metal NPs are synthesized by an inexpensive, simple and non-toxic, green methodology. Here, we have used the extract of lemon to reduce the manganese salt. 1 mmol of manganese salt solution was prepared freshly using manganese acetate salt.

The solution of lemon extracts (10 ml) was mixed with the aqueous solution of metal precursor with continuous stirring. The mixture was kept on magnetic hot stirrer for an hour, and the working temperature range was from 50°C to 60°C. When the metal precursor was added to the extracts, we observed drastic changes in color of the solution from pale green to pale yellow which indicated the reduction and formation of manganese NPs, where lemon extract acted as an effective reducing agent. Since the highly oxidation nature of manganese metal, the formed NPs were tending to form aggregation and this could be avoided by reacting with stabilizing agent. The stabilizing agent, i.e., curcumin extract (1 mm) was freshly prepared by dissolving in 95% ethanol, and the yellow colored solution was mixed with above manganese ion mixture. The solution temperature and pH were maintained at the same condition and stirring was continued for about 2 h to get complete stabilized NPs. The mixture color was changed slowly from yellowish to yellowish brown and then permanent reddish brown color. For betterment of the reaction, the variation of parameters - such as concentration of metal precursor, reducing and stabilizing agent, temperature, pH, and reaction time - were maintained at particular extend throughout the experiment. The obtained final colloid solution was centrifuged and washed several times with ethanol and water to obtain the pure MONP and kept in oven to dryness.

SC functionalized MONPs (MNSC)

Biofunctionalization of NPs is an advanced method of nanotechnology where the reaction is carried out by the normal interaction of biomaterial with NPs. Hence, the modified chitosan material was surface functionalized with synthesized MONPs. 1 mmol of the prepared SC was dissolved well in acetic acid and ethanolic mixture and kept on hot magnetic stirrer for an hour to get complete dissolved solution. To this hot solution, 1 mmol of above synthesized MONPs solution was mixed slowly, and the hot stirring was continued for 2-3 h. The color changes were observed first from the dark brown color to slow appearance of pale brown color which denoted the functionalization of SC with MONPs. The reaction mixture was centrifuged and washed several times with ethanol and double distilled water then kept to dryness for further analysis.

Biological assay

The antibacterial activity of the samples was evaluated by disc diffusion method of Bauer *et al*., 1966[51] against two Gram-positive bacteria (*S. aureus and B. subtilis*) and two Gram-negative bacteria (*E. coli and S. typhi*). In this analysis method, approximately, 2.0×10^6 colony-forming units (CFU/ml) of the bacterial cultures were prepared by diluting with autoclaved fresh Muller-Hinton broth medium and the prepared bacterial cultures were inoculated with synthesized NPs and standard antibiotic on Muller-Hinton agar plates. Then, the concentration of extracts is 40 mg/disc was loaded on 6 mm sterile disc and placed on the surface of the medium to get diffusion. The plates were kept for incubation at 37°C for 24 h. After incubation, the plates were studied for the presence of a zone of inhibition. Bactericidal activity with respect to zone of inhibition was also calculated using an antibiotic zone scale (HIMEDIA). Chloramphenicol was used as standard antibiotics for the pathogenic microorganism.

The antifungal activity was carried out by agar well diffusion method of Gomes *et al*., 2002,[52] against four funguses (*C. albicans*, *C. lunata*, *A. niger,* and *T. simii*). Approximately, 10^5 CFU/ml of inoculums were prepared using Sabouraud's dextrose agar (SDA) by suspending for 6 h. The sample of NPs with antibiotic and solvent blanks (SDA and acetic acid) was filled in the wells of the agar and fungal plates were incubated at 37°C for 72 h. Standard antibiotic, fluconazole (concentration 1 mg/ml) was used as positive control. The diameters of zone of inhibition observed were measured and studied.

RESULTS

Ultraviolet-visible (UV-Vis) studies

In general, formation of NPs and the stabilization were represented by a color changes observed during the reaction. The reduction of manganese metal salt was confirmed by the color change detected from pale green to pale yellow, and the stabilization of MONPs was detected by the color change from yellowish to permanent reddish brown color.

UV-Vis spectroscopy is the most convenient technique for the characterization of NPs. Formation and stability of NPs in aqueous colloidal solution is confirmed by UV-Vis spectral analysis. The UV-Vis absorption spectra of the synthesized MONP and biofunctionalized NPs were measured on a Shimadzu UV-Vis V-530A spectrophotometer in the range of 200-900 nm. Figures 1 and 2 show a UV-Vis spectrum of MONPs and SC functionalized manganese oxide NPs (MNSC), respectively. MONPs were exhibited a two important peaks at 360 nm and 215 nm which were exhibited as a small humps shown in Figure 1. Biofunctionalized MONPs showed two medium sharp peaks with noisy at around 339-341 nm and around 210-220 nm which were slightly lower in the wavelength compared with non-functionalized nanoform.

Fourier transform infrared (FTIR) studies

FTIR spectroscopy was carried out to find out the purity and nature of MONPs and biofunctionalized NPs synthesized by eco-friendly green synthesis method. In addition, it has shown the possible peaks responsible to functionalization of metal oxide NPs. The samples were examined on a Jasco FTIR/4100 spectrophotometer with 4/cm resolution in

the range of 4000-400/cm. Figures 3 and 4 show the FTIR spectrum of synthesized MONPs and biofunctionalized form, respectively. There was observed some common peaks in IR region for both MONP and MNSC are follows, respectively. 3650-3850/cm, 1704-1698/cm, 1574-1573/cm, 1393-1385/cm, and 1026-1160/cm, and below 1000 are the peaks exhibited for the same functional group present in both nanoformulations. Some of the different peaks were also realized in the IR spectral analysis which is important to express the formation of NPs and functionalization process discussed later.

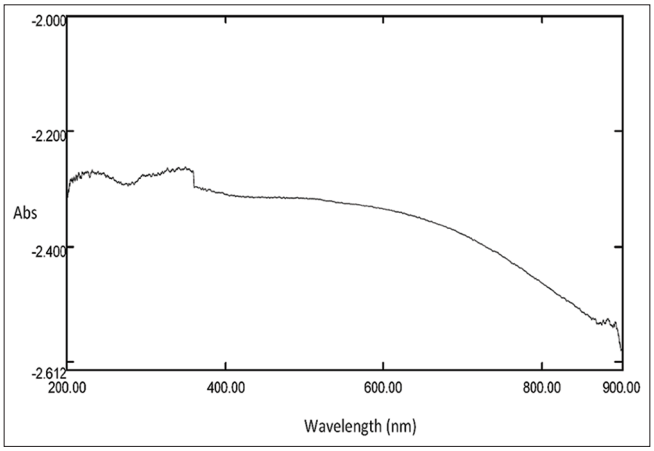

Figure 1: Ultraviolet-visible spectra of manganese oxide nanoparticle

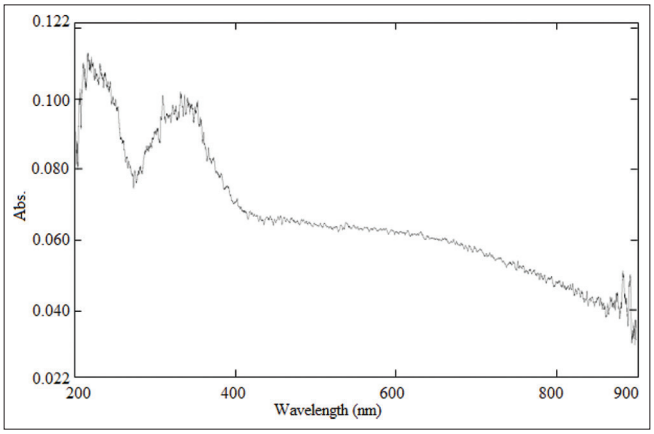

Figure 2: Ultraviolet-visible spectra of MNSC

Scanning electron microscopy (SEM) analysis

Morphology of synthesized MONPs and biofunctionalized form was characterized by SEM technique at different magnification levels. SEM images were recorded using JEOL Model JSM - 6390LV SEM. In general, in this analysis, the samples were placed in an evacuated chamber and scanned in a controlled pattern by an electron beam. Since the interaction of the electron beam with the samples produced a variety of physical phenomenon that detected and used to form images then provide information about the specimens. The SEM images of both nonfunctionalized and biofunctionalized NPs were shown in Figure 5a and b, respectively. Both nanoformulations were exposed the rough surfaced spherical and dot-shaped structures.

Transmission electron microscopy (TEM) analysis

However, to obtain a clear morphology and size of the NPs in depth the samples were analyzed using TEM. TEM analysis of both nanoformulations was carried out using a 300 kV JEOL-3011 instrument. Figure 6a and b shows the TEM images of the non-functionalized and biofunctionalized MONPs, respectively. Both nanoformulations were exhibited a spherical shaped morphology with affordable particle size.

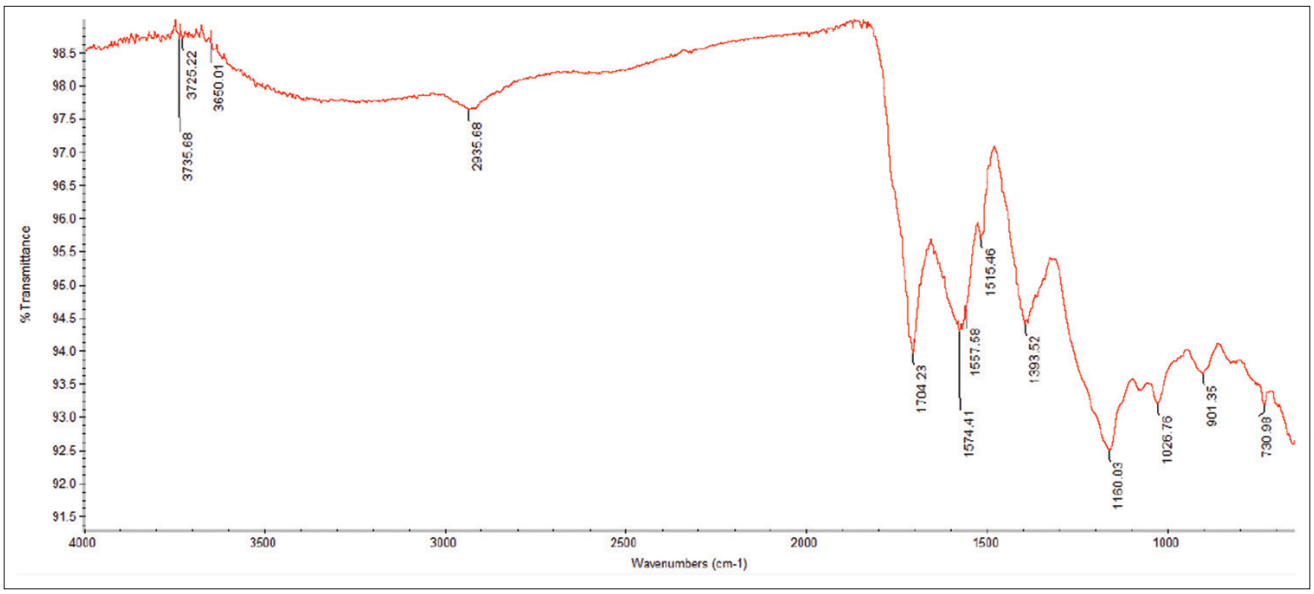

Figure 3: Fourier transform infrared spectra of manganese oxide nanoparticle

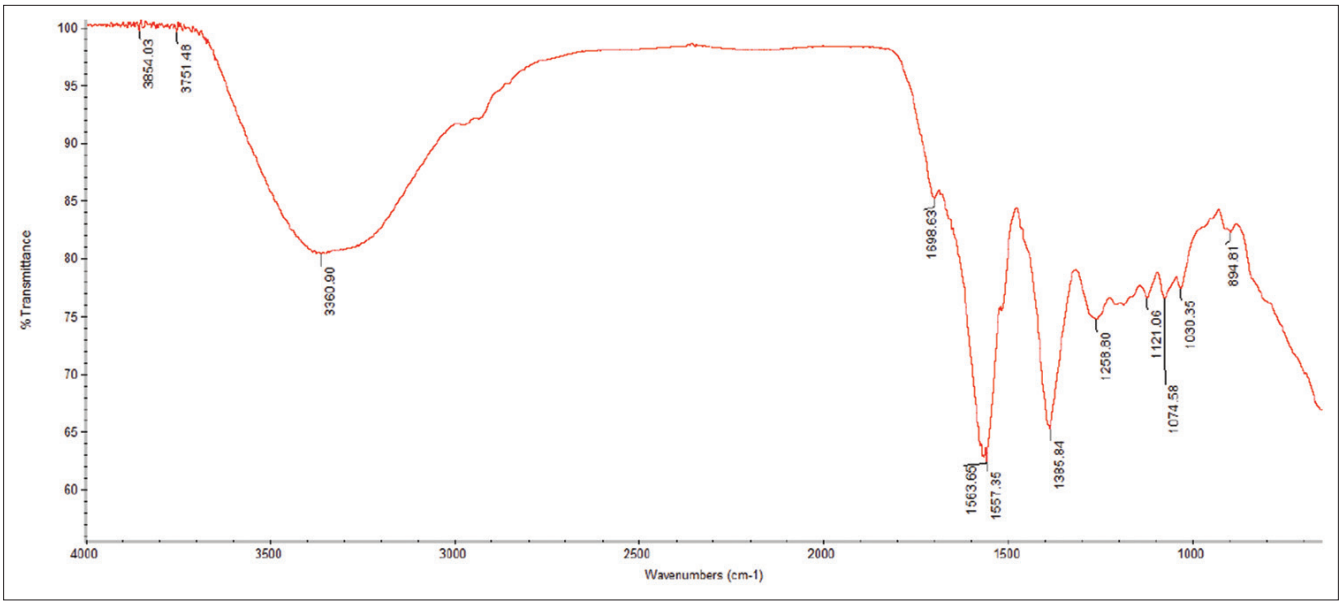

Figure 4: Fourier transform infrared spectra of MNSC

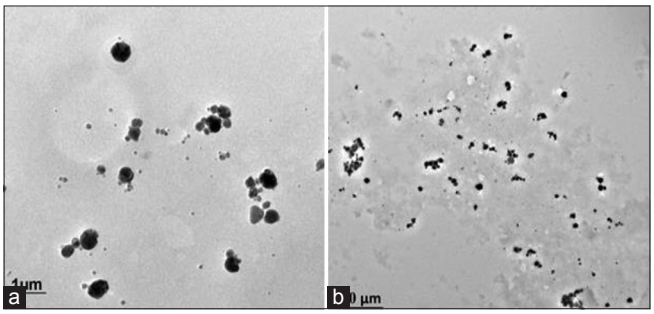

Figure 5: Scanning electron microscopy image of (a) Manganese oxide nanoparticle; (b) MNSC

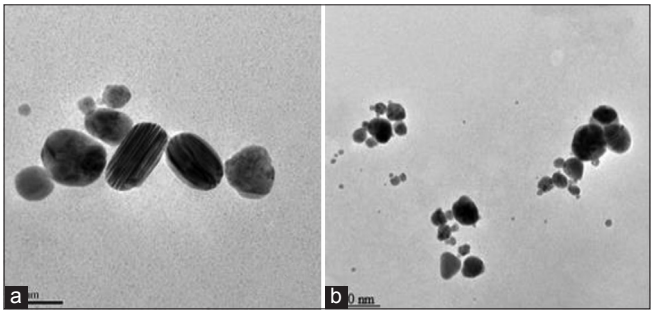

Figure 6: Transmission electron microscopy image of (a) Manganese oxide nanoparticle; (b) MNSC

Antibacterial assessment

The antibacterial activity of non-functionalized and SC functionalized MONPs was evaluated using disc diffusion method against two Gram-positive (*S. aureus* and *B. subtilis*) and two Gram-negative bacteria (*E. coli* and *S. typhi*). The results of activity were compared to a commercial antibiotic chloramphenicol [Table 1].

Antifungal assessment

The synthesized non-functionalized and SC functionalized MONPs were screened using agar well diffusion method for their antifungal activity against four fungal strains *C. albicans*, *C. lunata*, *A. niger,* and *T. simii*. The antifungal zone results were compared with standard antifungal drug fluconazole [Table 2].

DISCUSSION

Typically, NP formation mainly depends on the particular limits such as concentration of metal salt, reducer, and capping agent as well as reaction temperature and duration of reaction. The above-mentioned factors takes place a key role to determine the size and stability of produced NPs. The as synthesized NPs are characterized and detected by a various spectral analysis, however, the process of reduction of metal precursor as well as the stabilization of reduced metal NPs from oxidation or aggregation both can be established during the reaction itself by a simple and clear way of changes in color of the mixture which can be visible to naked eye. Moreover, from the visibility of color, the state of the reaction can be identified and facilitated to forward the reaction period. In our investigation, while the manganese precursor was mixed with the lemon extract, the reaction mixture produced pale green color initially. But during the reduction process of manganese metal, there was a color change observed rapidly from pale green to pale yellow. This could be due to the absorbed biomolecules of the extracts on the surface of the NPs allowed the particles to approach more closely and produced the smaller size of metal NPs. The reaction was continued with hot stirring for an hour but there was no considerable change in color, and

Table 1: Evaluation of antibacterial effectiveness using zone of inhibition test method

Bacterial species	Zone of inhibition diameter (mm sample^{-1})		
	C	MONP	MNSC
S. aureus	16	15	17
B. subtilis	13	08	13
E. coli	13	09	13
S. typhi	15	10	06

C: Standard drug; MONP: Manganese oxide nanoparticles, MNSC: Biofunctionalized manganese oxide nanoparticles, *S. aureus*: *Staphylococcus aureus*, *B. subtilis*: *Bacillus subtilis*, *E. coli*: *Escherichia coli* and *S. typhi*: *Salmonella typhi*

Table 2: Evaluation of antifungal effectiveness using zone of inhibition test method

Fungal species	Zone of inhibition diameter (mm sample^{-1})		
	C	MONP	MNSC
C. albicans	13	13	15
C. lunata	17	11	16
A. niger	13	11	14
T. simii	14	10	12

C: Standard drug, MONP: Manganese oxide nanoparticles, MNSC: Biofunctionalized manganese oxide nanoparticles, *C. albicans*: *Candida albicans*, *C. lunata*: *Curvularia lunata*, *A. niger*: *Aspergillus niger* and *T. simii*: *Trichophyton simii*

we have concluded that the metal precursor was reduced well since the formed small NPs were different from the substrate. Furthermore, manganese is a paramagnetic metal that oxidizes easily and resulting the highly agglomerated particles which may be reduce the bioactivity of MONPs. To avoid this troublesomeness, we have added the curcumin as a capping agent to produce reasonable size of NPs. In this step, there was a color change from yellowish to pale brown and in continuation with hot stirring, the final reaction mixture was exhibited a reddish brown color which revealed the formation of stabilized MONPs.

The UV absorption spectra of MONPs [Figure 1] exhibited the first peak at 360 nm was corresponding to the absorption maxima of MONPs and the second peak observed at 215 nm was probably due to the aggregation of formed NPs, which could be occurred by the oxidation of NPs and exhibited in the lower wavelength region. The absorption spectra of SC [Figure 2] displayed a medium sharp peak in the region of 339-341 nm which was assigned to the presence of MONPs. This could be observed in the lower region of wavelength due to the biofunctionalization of SC. Another one peak observed in the region of 210-220 nm was due to the NP agglomeration. However, the obtained two peaks were noisier due to some NP oxidation at surface of the formed MONPs.

The FTIR spectra of synthesized MONPs [Figure 3] have exhibited an important peak, where ensuring the presence of metal oxide NPs, reducing and stabilizing agent. From the data obtained, the peaks detected in the region of 3735-3650/cm could be assigned to the –OH (free) stretching of extract or ethanol present in the system. The weak broad band observed in the range of 2935/cm was due to the C-H stretching of capping agent curcumin. The C=O stretching of extract was observed at 1704/cm and three characteristic peaks in the range of 1574-1515/cm were ensuring the occurrence of aromatic unsaturation (C=C) of the stabilized curcumin system. The absorption peak at 1393/cm symbolized the C-H bending of adsorbed water of MONPs. The (C-O) stretching bands belongs to the curcumin was assigned by the peaks found at 1026/cm and 1160/cm and endorsing the presence of curcumin system well stabilized. In the case of SC functionalized MONPs [Figure 4], the various peaks observed in the IR region were similar to the non-functionalized NPs with slight deviations in wavelength due to the functionalization process. The peaks observed in the region of 3854-3751/cm can be designated to the O-H (free) stretching of extract or ethanol group present in the system. The actual broad peak detected in the region of 3360/cm may due to the stretching of O-H group lying in the aromatic system of SC. The major absorption bands observed by MNSC are followed. The C=O vibration band of acidic group of lemon extract was realized herein the lower region, at 1698/cm due to NPs functionalization, and the presence of aromatic C=C stretching of chitosan system was confirmed by the peak raised at 1563/cm. The important peaks raised at 1557/cm and 1385/cm which were belongs to the N-H bending and C-H bending of SC, respectively. The small broad peak observed at 1258/cm was due to the existence of C-O stretching of acidic group of lemon extract, and the consecutive three characteristic peaks observed in MNSC spectra in the region of 1121-1030/cm were owned to the stretching of C-H group of stabilized curcumin system. Metal oxides and hydroxides NPs generally absorption peak in the fingerprint region, i.e., below the wavelength of 1000/cm arising due to interatomic vibrations.[53] According to this, the significant absorption peaks observed in MONP at 901 cm^{-1}/730 cm^{-1} and exhibited in MNSC at 894/cm were corresponding to the characteristic stretching bands of O-Mn-O which represented the presence of the Mn-O metal stretching in the both non-functionalized and biofunctionalized MONPs.

The SEM image of synthesized MONPs [Figure 5a] has been exhibited a reasonable and clear morphology structure of formed NPs up to some extent. It has shown a small dot and spherical shaped morphology. Here, we could not find any aggregation of NPs. In the case of SEM image of SC functionalized MONPs [Figure 5b], the images were of small sized and different nanospherical morphology and exist in contact with each other. This could be due to the aggregation of particles.

The TEM micrograph image of the synthesized MONPs [Figure 6a] has showed that most of the NPs were spherical

in shape and some of eclipsed morphology with considerable particle size in the range of 50 nm. The TEM image of biofunctionalized MONPs [Figure 6b] was also exhibited a good spherical morphology structure, and the particle size was observed in the range about 40-60 nm and some of NPs nearly 100 nm. It is evident that there is variation in particle sizes of non-functionalized and biofunctionalized NPs clearly due to the particles were tending to agglomeration and resulting in the increment in the size of NPs. This few agglomerated MONPs were observed in some places, thereby indicating possible oxidation nature of paramagnetic manganese metal. However, our green methodology was produced relatively an appreciable result in terms of addition of supportive capping agent during the NP preparation.

The antibacterial activity of non-functionalized and biofunctionalized MONPs have been investigated by zone of inhibition method [Table 1]. The antibacterial activity results clearly represented that the zone of inhibition values against bacterial species produced by SC functionalized MONPs were significantly higher. The non-functionalized MONPs showed a moderate bactericidal activity against *S. aureus* only, and rest of those was very lower activity than standard drug and biofunctionalized form. However in the case of SC functionalized MONPs, the bacterial growth was inhibited enormously against both Gram-positive and Gram-negative bacterial species. The zone of inhibition test has showed an appreciable result carried out for the bacteriostatic test toward *S. aureus*, *B. subtilis,* and *E. coli* bacterial strains. The inhibition zone values were similar to the standard drug for *B. subtilis* and *E. coli* and this was higher than standard drug against *S. aureus*. It can be expressed that the presence of biomaterial, SC acted as a great role in the improvement of bioactivity. Therefore, we can conclude that biofunctionalized MONPs showed reasonably higher antibacterial activity than non-functionalized NPs due to the existence of SC.

The antifungal activity of non-functionalized and biofunctionalized MONPs have been assessed by agar well diffusion method [Table 2]. It is clear from the table results that the antifungal results of biofunctionalized MONPs have shown satisfactory improvement than the inhibition results observed by non-functionalized NPs. The non-functionalized NPs showed moderate antifungal activity toward *C. albicans* and *A. niger* fungal species. However, this was very lower than the biofunctionalized form. When compared to the antifungal result of SC functionalized MONPs, there was evidence that relatively high inhibition activity observed against overall pathogens. In particular, fungicidal activity toward *C. albicans* and *A. niger* was surprisingly higher than standard drug as well as non-functionalized form. MNSC showed comparatively good inhibition activity against *C. lunata*, which was almost similar to the activity of standard drug and we found satisfactory antifungal activity toward *T. simii*, although lower than the standard drug but higher than MONP.

As said earlier, the increase in the antibacterial and antifungal activity of SC functionalized MONPs is due to the fact that the existence of modified chitosan biomaterial. In general, MONPs showed a large surface-to-volume ratio which helps in strong binding with SC. Moreover, researchers are established the antimicrobial activity of chitosan very well. It showed reasonably high antimicrobial activity against microbes due to the reactive functional groups present in chitosan (amino group at the C2 position of each deacetylated unit and hydroxyl groups at the C6 and C3 positions) can be readily subjected to chemical derivatization allowing the manipulation of mechanical and solubility properties[54] enlarging its antimicrobial activity. In addition, the presence of azomethine group in the SC system can be developed a resistance against pathogenic strains would evidently increase largely. Therefore, our experiment results demonstrate that the increased antimicrobial activity of SC incorporated MONPs due to may be the three side mechanism of action for antibacterial activity such as bactericidal effect of NPs, the effect of cationic chitosan and biofunctionalization effect. From this investigation, we found that the functionalized biomaterial, i.e., SC acted as a key role in the increment of inhibition activity of biofunctionalized nano-form against bacterial and fungal pathogens than the non-functionalized MONPs as well as standard drugs.

CONCLUSION

In summary, this investigation has been performed to discover a new bioactive and cost-effective antimicrobial agent through a simple and nontoxic green biosynthesis method by utilizing plant materials. In which MONPs have been synthesized first using lemon extract as a reducer and turmeric curcumin extract as a stabilizing agent. In another hand, chitosan material was derived from prawn sample and used to prepare the biologically well active SC. Finally, bioactive SC was incorporated on the surface of the synthesized MONPs by biofunctionalization process. The spectral studies UV-vis and FTIR are ensured the formation and functionalization of NPs. SEM and TEM morphology studies are represented that the formed MONPs are of spherical and eclipsed morphology with size about 50 nm, and biofunctionalized NPs are of spherical morphology with size around 40-60 nm. The zone of inhibition activity results were revealed that SC functionalized nano-form have shown comparatively higher activity than non-functionalized MONPs as well as standard drugs toward *S. aureus*, *B. subtilis*, *E. coli* bacterial strains and *C. albicans, and A. niger* fungal species. Therefore, it may be concluded that the biofunctionalized MONPs have a higher biocidal effectiveness in resisting bacterial growth, thus our findings reveals that SC possess a great role in the antimicrobial activity increment of the synthesized MONPs while it was surface functionalized with them. This may lead to propose valuable inventions in the field of antimicrobial systems as well as other medical applications in the future.

ACKNOWLEDGMENTS

We thank AMET University, Chennai, India, for their support to do this work. We gratefully acknowledge SAIF, North-Eastern Hill University (NEHU), Shillong for TEM analysis and Nanotechnology Research Centre, SRM University, Chennai for SEM analysis facility.

REFERENCES

1. Salem W, Leitner DR, Zingl FG, Schratter G, Prassl R, Goessler W, *et al.* Antibacterial activity of silver and zinc nanoparticles against Vibrio cholerae and enterotoxic Escherichia coli. Int J Med Microbiol 2015;305:85-5.
2. Lewis K, Klibanov AM. Surpassing nature: Rational design of sterile-surface materials. Trends Biotechnol 2005;23:343-8.
3. Rosi NL, Mirkin CA. Nanostructures in biodiagnostics. Chem Rev 2005;105:1547-62.
4. Logeswari P, Silambarasan S, Jayanthi A. Synthesis of silver nanoparticles using plants extract and analysis of their antimicrobial property. J Saudi Chem Soc 2015;19:311-7.
5. Burda C, Chen X, Narayanan R, El-Sayed MA. Chemistry and properties of nanocrystals of different shapes. Chem Rev 2005;105:1025-102.
6. Thill A, Zeyons O, Spalla O, Chauvat F, Rose J, Auffan M, *et al.* Cytotoxicity of CeO2 nanoparticles for *Escherichia coli*. Physico-chemical insight of the cytotoxicity mechanism. Environ Sci Technol 2006;40:6151-6.
7. Apperlot G, Lipovsky A, Dror R, Perkas N, Nitzan Y, Lubart R, *et al*. Enhanced antibacterial activity of nanocrystalline ZnO due to increased ROS-mediated cell injury. Adv Funct Mater 2009;19:842-52.
8. Shankar B, Krishnan S, Vasantha M, Arun B, Williams PH. Outer membrane proteins of wild-type and intimin-deficient enteropathogenic *Escherichia coli* induce Hep-2 cell death through intrinsic and extrinsic pathways of apoptosis. Int J Med Microbiol 2009;299:121-32.
9. King RB, Rodriguez JA, Fernandez-Garcia M, editors. Synthesis, Properties and Applications of Oxide Nanoparticles. New Jersey: Wiley; 2007. p. 733.
10. Hajipour MJ, Fromm KM, Ashkarran AA, Jimenez de Aberasturi D, de Larramendi IR, Rojo T, *et al.* Antibacterial properties of nanoparticles. Trends Biotechnol 2012;30:499-511.
11. Wei W, Cui X, Chen W, Ivey DG. Manganese oxide-based materials as electrochemical supercapacitor electrodes. Chem Soc Rev 2011;40:1697-721.
12. Song MK, Zhang Y, Cairns EJ. A long-life, high-rate lithium/sulfur cell: A multifaceted approach to enhancing cell performance. Nano Lett 2013;13:5891-9.
13. Li WN, Yuan JK, Gomez-Mower S, Xu LP, Sithambaram S, Aindow M, *et al.* Hydrothermal synthesis of structure-and shape-controlled manganese oxide octahedral molecular sieve nanomaterials. Adv Funct Mater 2006;16:1247-53.
14. Chen H, He J. Facile synthesis of monodisperse manganese oxide nanostructures and their application in water treatment. J Phys Chem C 2008;112:17540-5.
15. Jayandran M, Haneefa MM, Balasubramanian V. Facile green synthesis of iron nanoparticles using natural reducer and stabilizer and an evaluation of antimicrobial activity. Int J Adv Sci Tech Res 2015;5:62-70.
16. Stoia M, Muntean C, Militaru B. Fine $MnFe_2O_4$ nanoparticles for potential environmental applications. J Therm Anal Calorim 2015;121:1003-10.
17. Xiao W, Wang D, Lou XW. Shape-controlled synthesis of MnO_2 nanostructures with enhanced electrocatalytic activity for oxygen reduction. J Phys Chem C 2010;114:1694-700.
18. Ching S, Welch EJ, Hughes SM, Bahadoor AB, Suib SL. Nonaqueous sol-gel syntheses of microporous manganese oxides. Chem Mater 2002;14:1292-9.
19. Wang N, Cao X, He L, Zhang W, Guo L, Chen C, *et al*. One-pot synthesis of highly crystallined λ-MnO_2 nanodisks assembled from nanoparticles: Morphology evolutions and phase transitions. J Phys Chem C 2008;112:365-9.
20. Yu XQ, He Y, Sun JP, Tang K, Li H, Chen LQ, *et al.* Nanocrystalline MnO thin film anode for lithium ion batteries with low over potential. Electrochem Commun 2009;11:791-4.
21. Ahmad T, Ramanujachary KV, Lofland SE, Ganguli AK. Nanorods of manganese oxalate: A single source precursor to different manganese oxide nanoparticles (MnO, Mn_2O_3, Mn_3O_4). J Mater Chem 2004;14:3406-10.
22. Banis MN, Zhang Y, Banis HN, Li R, Sun X, Jiang X, *et al.* Controlled synthesis and characterization of single crystalline MnO nanowires and Mn-Si oxide heterostructures by vapor phase deposition. Chem Phys Lett 2011;501:470-4.
23. Kumar H, Manisha A, Sangwan P. Synthesis and characterization of MnO_2 nanoparticles using co-precipitation technique. Int J Chem Chem Eng 2013;3:155-60.
24. Baykal A, Kavas H, Durmuş Z, Demir M, Kazan S, Topkaya R, *et al.* Synthesis and chracterization of Mn_3O_4 nanoparticles. Cent Eur J Chem 2010;8:633-8.
25. Pemartin K, Solans C, Alvarez-Quintana J, Sanchez-Dominguez M. Synthesis of Mn-Zn ferrite nanoparticles by the oil-in-water microemulsion reaction method. Colloids Surf A 2014;451:161-71.
26. Ramalakshmi M, Shakthivel P, Kim M. Mn_3O_4 nanoparticle synthesis via ionic liquid-assisted route. J Supercond Nov Magn 2014;27:2595-8.
27. Thakkar KN, Mhatre SS, Parikh RY. Biological synthesis of metallic nanoparticles. Nanomed Nanotechnol Biol Med 2010;6:257-62.
28. Abdel-Aziz MS, Shaheen MS, El-Nekeety AA, Abdel-Wahhab MA. Antioxidant and antibacterial activity of silver nanoparticles biosynthesized using Chenopodium

murale leaf extract. J Saudi Chem Soc 2014;18:356-63.
29. Ravichandran V, Xin TZ, Subashini G, Xiang TF, Yang EF, Jeyakumar N, *et al*. Biosynthesis of silver nanoparticles using mangosteen leaf extract and evaluation of their antimicrobial activities. J Saudi Chem Soc 2011;15:113-20.
30. Nadagouda MN, Castle AB, Murdock RC, Hussain SM, Varma RS. *In vitro* biocompatibility of nanoscale zerovalent iron particles (NZVI) synthesized using tea polyphenols. Green Chem 2010;12:114-22.
31. Siavash I. Green synthesis of metal nanoparticles using plants. Green Chem 2011;13:2638-50.
32. Jha AK, Prasad K. Facile green synthesis of metal and oxide nanoparticles using papaya juice. J Bionanosci 2015;9:311-4.
33. Chatterjee AK, Sarkar R, Chattopadhyay AP, Pulakesh A, Chakraborty R, Tarakdas B. A simple robust method for synthesis of metallic copper nanoparticles of high antibacterial potency against *E. coli*. Nanotechnology 2012;23:85103.
34. Kumar SS, editor. Biological and Pharmaceutical Nanomaterials. 1st ed. Weinheim: Wiley-VCH Verlag GmbH Co., KGaA; 2005.
35. Veiseh O, Gunn JW, Zhang M. Design and fabrication of magnetic nanoparticles for targeted drug delivery and imaging. Adv Drug Deliv Rev.2010;62:284-304.
36. Katz E, Willner I. Integrated nanoparticle–biomolecule hybrid systems: Synthesis, properties and applications. Angew Chem Int Ed Engl 2004;43:6042-108.
37. Marie-Alexandra N, Ulrich S. Surface modification and functionalization of metal and metal oxide nanoparticles by organic ligands. Monatsh Chem 2008;139:183-95.
38. Sevda S, Susan JM. Potential applications of chitosan in veterinary medicine. Adv Drug Deliv Rev 2004;56:1467-80.
39. Goy RC, Britto D, Assis OB. A review of the antimicrobial activity of chitosan. Polimeros 2009;19:241-7.
40. Lifeng Q, Zirong X, Xia J, Caihong H, Xiangfei Z. Preparation and antibacterial activity of chitosan nanoparticles. Carbohydr Res 2004;339:2693-700.
41. Chung YC, Chen CY. Antibacterial characteristics and activity of acid-soluble chitosan. Bioresour Technol 2008;99:2806-14.
42. Katsori AM, Chatzopoulou M, Dimas K, Kontogiorgis C, Patsilinakos A, Trangas T, *et al.* Curcumin analogues as possible anti-proliferative and anti-inflammatory agents. Eur J Med Chem 2011;46:2722-35.
43. Tharakan ST, Inamoto T, Sung B, Aggarwal BB, Kamat AM. Curcumin potentiates the antitumor effects of gemcitabine in an orthotopic model of human bladder cancer through suppression of proliferative and angiogenic biomarkers. Biochem Pharmacol 2010;79:218-28.
44. Ghosh D, Choudhury ST, Ghosh S, Mandal AK, Sarkar S, Ghosh A, *et al*. Nanocapsulated curcumin: Oral chemopreventive formulation against diethylnitrosamine induced hepatocellular carcinoma in rat. Chem Biol Interact 2012;195:206-14.
45. Garcia OB, Castillo J, Marin JR, Ortuno A, Rio JA. Uses and properties of citrus flavonoids. J Agric Food Chem 1997;45:4505-15.
46. Vinson JA, Su X, Zubik L, Bose P. Phenol antioxidant quantity and quality in foods: Fruits. J Agric Food Chem 2001;49:5315-21.
47. Manjunath MN, Sattigeri VD, Nagaraj KV. Curcumin in turmeric. Spice India 1991;4:7-9.
48. Brine J, Austin R. Chitin isolates-species variation in residual amino acids. Comp Biochem Physiol B Biochem Mol Biol 1981;70:173-8.
49. Muzzarelli RA, Jeuniaux C, Gooday GW, editors. Chitin in Nature and Technology. New York, USA: Plenum; 1986.
50. Jayandran M, Haneefa MM. Synthesis characterization and biological activities of chitosan based schiff base complex. Chem Sci Rev Lett 2014;3:1050-9.
51. Gomes BP, Ferraz CC, Vianna ME. *In vitro* antimicrobial activity of Ca $(OH)_2$ pastes and their vehicles against selected microorganisms. Braz Dent J 2002;13:155-61.
52. Bauer RW, Kirby MD, Sherris JC, Turck M. Antibiotic susceptibility testing by a standard single disc method. Am J Clin Pathol 1966;45:493-6.
53. Kang L, Zhang M, Liu ZH, Ooi K. IR spectra of manganese oxides with either layered or tunnel structures. Spectrochim Acta A Mol Biomol Spectrosc 2007;67:864-9.
54. Giri MN, Agarwala V. Synthesis and characterization of novel magnetic chitosan bead and their antibacterial applications. J Bionanosci 2015;9:276-80.

Source of Support: Nil. **Conflict of Interest:** None declared.